Polymer Journal (2019) 51:1163–1172
https://doi.org/10.1038/s41428-019-0226-z

ORIGINAL ARTICLE

Relaxation behavior of random copolymers containing rigid fumarate and flexible acrylate segments by dynamic mechanical analysis

Yasuhito Suzuki[1] · Tomoya Tsujimura[1] · Kenji Funamoto[1] · Akikazu Matsumoto[1]

Received: 15 February 2019 / Revised: 5 June 2019 / Accepted: 6 June 2019 / Published online: 2 July 2019

Abstract

Due to the absence of a methylene spacer in the main chain, poly(substituted methylene)s with rigid structures possess some distinguished properties including a unique β-relaxation process. In this study, two series of random copolymers of diisopropyl fumarate (DiPF) with 1-adamantyl acrylate (AdA) and *n*-butyl acrylate (nBA) with various compositions were synthesized. The relaxation behavior of the copolymers was investigated using dynamic mechanical analysis (DMA) and differential scanning calorimetry (DSC). The α-relaxation temperature of the copolymers decreased as the acrylate content increased. Depending on the glass transition temperature (T_g) of the counterpart copolymers, that is, $T_g = 156$ °C for the homopolymer of AdA and $T_g = -53$ °C for the homopolymer of nBA, the β-relaxation temperature from the DiPF segments systematically shifted. While the β-relaxation temperature increased when copolymerized with AdA, the temperature decreased when copolymerized with nBA. Both copolymers maintained a high storage modulus of more than 10 MPa in the range between the α- and β-relaxation temperatures. The merging of the α and β processes at an intermediate composition was also observed. The random copolymerization of DiPF and acrylates enables us to fine tune the properties associated with the β-relaxation of DiPF segments.

Introduction

Because of well-developed synthetic methods, the properties of poly(monosubstituted ethylene)s (vinyl polymers) have been widely investigated. Controlling the chemical structure of side groups enables us to fine tune physical properties. For example, the glass transition temperature (T_g) of poly(alkyl methacrylate)s can be controlled from –70 °C to 111 °C simply by varying the length of alkyl side chains [1]. The manipulation of the glass transition is equivalent to the control of the α-relaxation process [2]. The effectiveness of random copolymerization to control the physical properties has been reported [3].

In contrast to vinyl polymers, research regarding poly(1,2-disubstituted ethylene)s, that is, poly(substituted methylene)s, is limited [4, 5]. The extremely low propagation kinetics originating from steric hindrance prevents the polymerization in many cases. An exception is the radical polymerization of some dialkyl fumarates [6–8]. When the ester alkyl group of the fumarate is bulky, a high-molecular-weight poly(dialkyl fumarate) can be synthesized [4, 9]. Polymers are produced when not only the propagation rate but also the termination rate becomes reasonably slow. A fundamental difference between poly(monosubstituted ethylene)s and poly(1,2-disubstituted ethylene)s is whether or not a methylene spacer (–CH_2–) in the main chain is present. Due to the absence of a methylene spacer, poly(dialkyl fumarate) forms a rigid chain structure with high rotational energy [10–13].

It is well known that typical amorphous polymers exhibit a main α-relaxation and a weaker β-relaxation process [14]. These relaxation processes can be observed by dielectric spectroscopy (DS) [15], mechanical analysis [16], thermal analysis [17], solid-state nuclear magnetic resonance (NMR) spectroscopy [18], friction force microscopy [19], and fluorescence microscopy [20]. It is noteworthy that the detailed and fundamental mechanisms of both the α- and

Supplementary information The online version of this article (https://doi.org/10.1038/s41428-019-0226-z) contains supplementary material, which is available to authorized users.

✉ Akikazu Matsumoto
matsumoto@chem.osakafu-u.ac.jp

[1] Department of Applied Chemistry, Graduate School of Engineering, Osaka Prefecture University, 1-1 Gakuen-cho, Naka-ku, Sakai, Osaka 599-8531, Japan

β-relaxations are not perfectly understood despite a large amount of knowledge about these relaxations [21]. A simple view of α- and β-relaxations for amorphous polymers correlates these dynamics to the segmental dynamics of the main chain and the local motion of the side group, respectively [14]. However, this simple picture does not always apply, especially for rigid molecules [21]. It was revealed that α- and β-relaxations are not fully independent [18]. Some β-relaxations are considered to be a local step of the α-segmental relaxation [21]. In the case of poly(methyl methacrylate) (PMMA), a detailed analysis by NMR spectroscopy showed that the side-group flip correlates with the main chain rearrangement [22]. Based on the results of the dynamic mechanical analysis (DMA) of poly(diisopropyl fumarate) (PDiPF) film, Yamada et al. reported a change in the storage modulus from ~1 GPa to ~0.1 GPa ca. 100 °C, which corresponded to the β-relaxation [23]. They also pointed out that the observed intensity of the α-relaxation was much smaller than that of the β-relaxation. Kurosu et al. investigated the chain dynamics of PDiPF in solid-state ^{13}C cross-polarized magic angle spinning and ^{1}H pulse NMR spectroscopic experiments [24]. They revealed that the reorientation frequency of the main chain of PDiPF was 42.6 kHz at 120 °C and that the molecular motion was highly restricted by an increase in the bulkiness of the ester alkyl group.

Previous research has clarified unique properties of PDiPF, including gas permeation [25], surface properties [26], solution properties [10–13], solid-state chain dynamics [23, 24], liquid crystals [27–29], and electro-optical properties [30–32]. At least some of these unique properties are intimately related to relaxation processes [25]. Thus, it is of great importance to control and understand the relaxation behavior of PDiPF. In this study, we synthesized random copolymers of diisopropyl fumarate (DiPF) with two different alkyl acrylates, that is, 1-adamantyl acrylate (AdA) and *n*-butyl acrylate (nBA). While the T_g of poly(*n*-butyl acrylate) (PnBA) is –53 °C, that of poly(1-adamantyl acrylate) (PAdA) is 156 °C [33]. We discuss the shift in relaxation temperatures and the merging of the α- and β-relaxations as a function of the copolymer composition.

Experimental methods

Materials

DiPF (Fujifilm Wako Pure Chemical Corporation, Tokyo, Japan) and nBA (Tokyo Chemical Industry Corporation, Ltd, Tokyo, Japan) were distilled under reduced pressure prior to use. Dimethyl 2,2′-azobis(2-methylpropionate) (MAIB, Fujifilm Wako Pure Chemical Corporation, Tokyo, Japan) was purified via recrystallization in *n*-hexane before use. AdA was provided by Osaka Organic Chemical Industry Ltd, Osaka, Japan and was purified via recrystallization in *n*-hexane before use.

Synthesis of random copolymers

Here, the synthetic methods are briefly summarized. The detailed synthetic methods of the homopolymers and random copolymers of DiPF are reported elsewhere [33, 34]. DiPF, an acrylate (nBA or AdA), and MAIB were mixed in a polymerization tube. Freeze–pump–thaw cycles were repeated three times for degassing. Under a nitrogen atmosphere, the polymerization was conducted at 60 °C for nBA or 80 °C for AdA. The obtained polymer was dissolved in chloroform and subsequently precipitated in an excess amount of a methanol/water mixture (9/1 vol/vol). The polymer was washed with the methanol/water mixture and collected by decantation or percolation. The polymer was dried under vacuum at 60 °C. The precipitation process was repeated twice for purification.

Measurements

^{1}H NMR spectra were recorded using ECS-400 and ECX-400 spectrometers (JEOL, Tokyo, Japan). Size exclusion chromatography (SEC) was employed to elucidate the number-average (M_n) and weight-average (M_w) molecular weights. Tetrahydrofuran (flow rate 0.8 mL/min) was used as the eluent at 40 °C. The SEC system was developed with a PU-2080-Plus (pump), a DG-2080-53 (degasser), an RI-2031-Plus (RI detector), and a UV-2031-Plus (UV detector, 300 nm) (JASCO, Tokyo, Japan). TSK gel GMHHR-N (Tosoh Corporation Ltd, Tokyo, Japan) was used as the column. The molecular weights were calibrated against standard polystyrenes (Tosho Corporation Ltd, Tokyo, Japan). Thermogravimetric (TG) analysis was conducted using a DTG-60 (Shimadzu Corporation Ltd, Kyoto, Japan) with a scanning rate of 10 °C/min under a nitrogen atmosphere. Differential scanning calorimetry (DSC) was measured using a DSC-60 (Shimadzu Corporation Ltd, Kyoto, Japan) under nitrogen flow with a scanning rate of 10 °C/min.

Samples for DMA were prepared by thermal welding. Approximately 1.5 g of the polymer was inserted in a rectangular mold (5 cm × 1 cm). After the polymer was annealed for 30 min at 150 °C, pressure (approximately 1 MPa) was applied for 1 h at the same temperature. Typically, a rectangular sample with a thickness of 2 mm was obtained. A DMS 6100 (Seiko Instruments Inc., Tokyo, Japan) was utilized for the DMA measurement. The instrument was operated in dual cantilever mode with a heating rate of 2 °C/min. Sinusoidal strains with an amplitude of 10 μm at 2 Hz was applied. DMA data for some

polymers was collected at five different frequencies in a range of 0.5–10 Hz.

Results and discussion

In this study, three kinds of homopolymers, PDiPF, PnBA, and PAdA, as well as the random copolymers of DiPF with nBA [P(DiPF-*co*-nBA)] and of DiPF with AdA [P(DiPF-*co*-AdA)], were synthesized based on the procedure reported previously [33, 34]. The schematic poly(1,2-disubstituted ethylene) [i.e., poly-(substituted methylene)] and poly (monosubstituted ethylene), as well as the structures of PDiPF, PnBA, and PAdA, are displayed in Fig. 1. PDiPF was selected as a model poly(1,2-disubstituted ethylene) because of the relatively high polymerization reactivity of the corresponding monomer. To obtain high-molecular-weight polyfumarates, the ester alkyl groups need to be bulky because such monomers have reasonably slow termination rates that compensate for the slow propagation rate [35–37]. For example, the reaction of dimethyl fumarate only produces oligomers because the methyl group is not bulky enough. In contrast, previous studies showed that the polymerization of DiPF proceeds to give high-molecular-weight polymers via bulk polymerization or in solution. Among the polyfumarates, the physical properties of PDiPF have been well investigated [10–13, 27–32]. AdA and nBA were selected as acrylates in this study. Adamantane has a rigid symmetrical structure with a high melting point (270 °C). Typically, the insertion of adamantyl groups in the polymer main and side chains increases the T_g of the polymers [33, 34, 38–45]. Due to the side-chain structure, the T_g values of PnBA and PAdA are –53 °C and 156 °C, respectively [33].

Representative ^{1}H NMR spectra of P(DiPF-*co*-nBA) and P(DiPF-*co*-AdA) are shown in Fig. 2. The signal from the proton denoted as b in the schematic as well as the proton denoted as f in the case of P(DiPF-*co*-nBA) or other protons in the case of P(DiPF-*co*-AdA) were used to determine the copolymer composition. The characteristics of the copolymers prepared in this study are summarized in Table 1. The higher the acrylate composition is, the broader the dispersity (M_w/M_n) becomes. This is due to the reactivity differences between DiPF and acrylates. In our previous study, monomer reactivity ratios and the number-average sequence lengths for DiPF and AdA were calculated [34]. Five different copolymers whose DiPF composition spanned from 3 to 59 mol% were analyzed. The number-average sequence lengths of DiPF and AdA ranged from 1.01 to 2.44 and 1.69 to 30.7, respectively. This result suggests that the DiPF sequence is randomly well distributed for all the analyzed copolymers. In other words, the probability of a long DiPF sequence in the copolymer was low for the copolymers produced under the conditions used in the previous and present studies. T_{d5} was determined from the 5% weight loss in the TG curves. The decomposition of an isopropyl ester group in PDiPF occurs at the lowest temperature [34]. As the DiPF content in copolymer decreased, T_{d5} increased.

Figure 3 shows the DMA results for the homopolymers. Figure 3a displays the storage and loss moduli of PAdA observed at 2 Hz as a function of temperature. Because of the adamantyl moiety in the side chain, the T_g of PAdA is higher than typical polyacrylates [2]. The storage modulus was almost the same below the onset of the α-relaxation

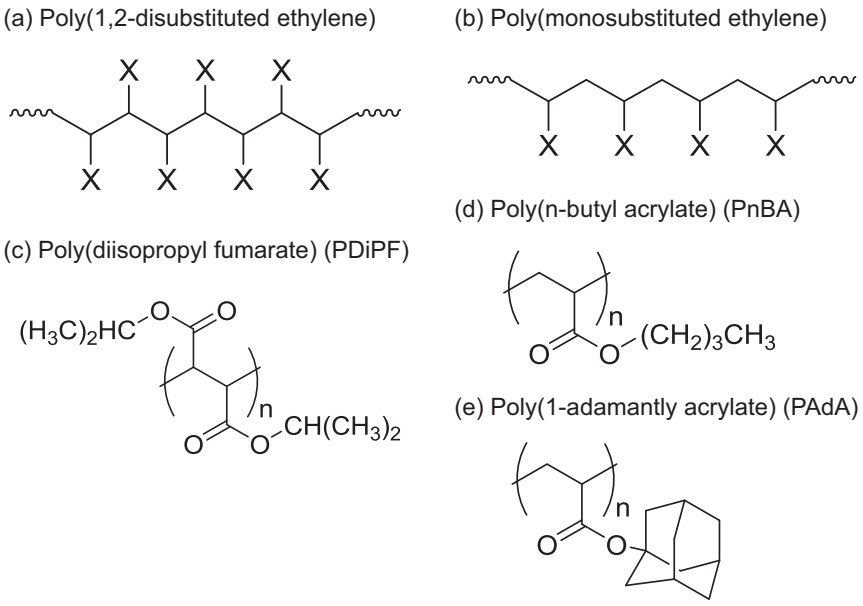

Fig. 1 Schematics of **a** poly(1,2-disubstituted ethylene) and **b** poly(monosubstituted ethylene). Structures of **c** poly(diisopropyl fumarate) (PdiPF), **d** poly(*n*-butyl acrylate) (PnBA), and **e** poly(1-adamantyl acrylate) (AdA) are provided

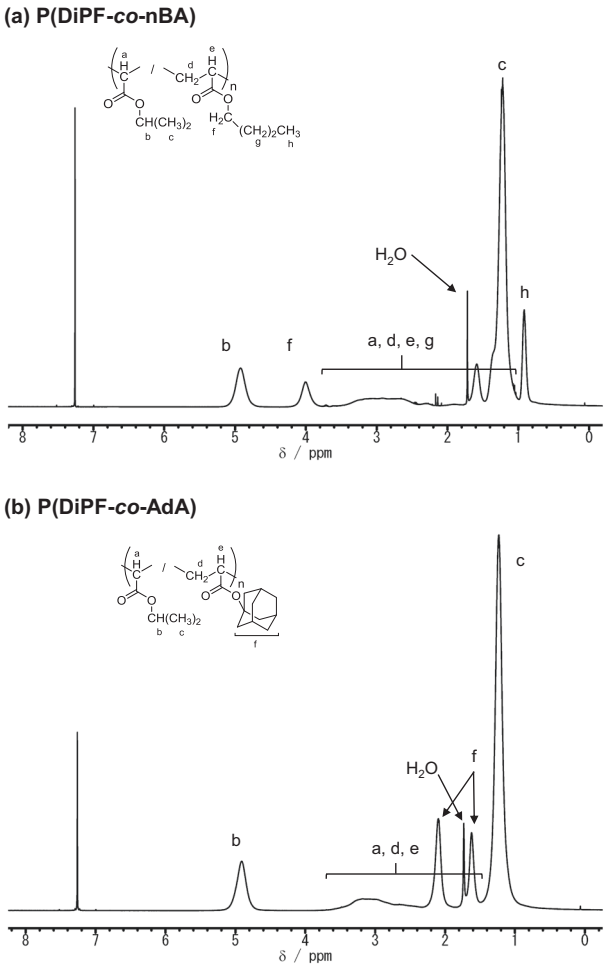

Fig. 2 ^{1}H nuclear magnetic resonance (NMR) spectra of **a** P(DiPF-*co*-nBA) and **b** P(DiPF-*co*-AdA). Based on the ratio between the signal from the proton denoted as b and other protons, the DiPF content was calculated to be 64 mol% and 76 mol% for **a**, **b**, respectively

process at approximately 140 °C. Then, the storage modulus suddenly decreased from ~1 GPa to ~10 kPa. At temperatures above the α-relaxation, the polymer was rubbery. The peak temperature of the loss modulus for PAdA shown in Fig. 3a was 151.4 °C and is a good indication of the segmental motion. The slight decrease in the storage modulus ca. −100 °C indicates the existence of the β-process (see Fig. S1 in the Supporting Information). In any case, the intensity of the β-process was much smaller than that of the α-process. This behavior was qualitatively similar to other vinyl polymers such as PMMA [46]. Compared to the data of PAdA, the DMA curve of PDiPF was fundamentally different (Fig. 3c). Two relaxation processes were observed at 73.4 °C and ca. 215 °C as the peaks of the loss moduli (Fig. 3c). The processes were also confirmed from the peaks of the tan δ (Fig. 3d). During the lower temperature relaxation, the storage modulus decreased from 1.3 GPa at 50 °C to 0.2 GPa at 100 °C. Although the relaxation process is clear, the absolute value of storage modulus (0.2 GPa) indicates that the sample is still glassy, that is, a nonfluid solid. The storage modulus in a range between the low- and high-temperature relaxations was more or less constant. The intensity of the higher temperature process was weak. In this study, the measurement was stopped at 230 °C to avoid the decomposition of the sample. Consistent with previous reports [23], it is reasonable to assign the high- and low-temperature processes to the α- and β-relaxations, respectively. The α-relaxation of PDiPF was observed ca. 220 °C, which was close to the onset temperature of thermal decomposition. Therefore, we checked the relaxation processes for another fumarate polymer. The relaxation processes of poly(diethyl fumarate) (PDEF) were detected at 18.9 °C and 159.4 °C, which were assigned to the β- and α-relaxations, respectively (Fig. 3e, f). Both relaxation temperatures for PDEF were lower than those for PDiPF because the steric bulkiness of the ester in the side chain was small. As discussed later, the low-temperature relaxation process of the polyfumarates possesses unusual characteristics.

Selected DMA curves of PDiPF and P(DiPF-*co*-AdA)s with different compositions are displayed in Fig. 4a. As discussed earlier, the storage modulus of PDiPF stayed approximately 0.2 GPa above the β-relaxation temperature at 73.4 °C. As the composition of the DiPF units decreased, the storage modulus after the β-relaxation decreased more significantly. In the case of P(DiPF-*co*-AdA)-46, the storage modulus at 180 °C was approximately 0.6 MPa. The shift in relaxation temperatures is discussed with respect to the tan δ presented in Fig. 4b. The α- and β-relaxation of PDiPF are indicated in Fig. 4. Comparing the results from PDiPF, P(DiPF-*co*-AdA)-89, and P(DiPF-*co*-AdA)-76, the β-relaxation temperature increased as the composition of DiPF decreased. In many cases, β-relaxation is a very local motion of the side groups [21]. The fact that the β-relaxation temperature shifted along with the copolymer composition in the present study implies the local dynamics of the side chains are influenced by the sequence structure of the main chain. In contrast to an increase in the β-relaxation temperature, the α-relaxation temperature decreased as the composition of DiPF decreased. The broad α-relaxation may reflect the statistical distribution of the successive DiPF segments. Interestingly, these two processes seemed to merge in the case of P(DiPF-*co*-AdA)-46, resulting in the observation of an apparent single relaxation process with a high intensity of the tan δ peak.

Similarly, the DMA results of P(DiPF-*co*-nBA)s with different compositions are shown in Fig. 5a. Because of the flexible alkyl side group, the T_g of PnBA was –53 °C. Again, as the acrylate composition increased, the storage modulus above the β-relaxation temperature decreased. While the storage modulus was almost constant in the case of PDiPF between the α- and β-relaxation temperatures, the

Table 1 List of homopolymers and random copolymers synthesized in this study

Acrylate	DiPF/Acrylate (mol/mol)		Temp. (°C)	Time (h)	Yield (%)	M_w /10^4	M_w/M_n	T_{d5} (°C)	T_{DSC}[a] (°C)	T_β[b] (°C)	Tan δ peak temp.[c] (°C)	E_{act}[d] (kJ/mol)
	In feed	In copolymer										
AdA	100/0	100/0	60	7	47	12	1.5	267	66	73.4	218, 84	270
	95/5	89/11	60	2	36	27	1.9	253	70	86.3	198, 101	310
	90/10	76/24	60	2	45	31	2.2	273	83	98.5	150, 113	–
	85/15	65/35	60	1	39	32	2.3	286	105	–	148, 120	–
	70/30	46/54	60	1.5	45	30	3.1	289	114	115.7	139	–
	0/100	0/100	60	1	96	25	1.5	358	156	–	182	290
nBA	95/5	95/5	80	3	81	9.3	1.8	258	62	59.0	207, 72	280
	90/10	89/11	80	3	78	11	1.7	263	66	–	203, 76	290
	80/20	78/22	80	3	77	7.6	1.8	252	58	64.3	203, 73	290
	70/30	64/36	80	3	72	7.6	2.1	273	0	16.0	84, 30	–
	50/50	35/65	80	1	50	11	2.7	286	–17	–	–	–
	30/70	19/81	80	1	48	18	4.5	282	–53	–	–	–

DSC differential scanning calorimetry, *DMA* dynamic mechanical analysis, *DiPF* diisopropyl fumarate, *AdA* 1-adamantyl acrylate, *nBA* *n*-butyl acrylate

[a]Determined by DSC

[b]Determined from loss modulus by DMA at a frequency of 2 Hz

[c]Determined from tan δ by DMA at a frequency of 2 Hz

[d]Estimated from tan δ measured with five different frequencies (0.5, 1, 2, 5, and 10 Hz)

storage modulus slightly decreased as the fraction of DiPF units decreased. For PDiPF, P(DiPF-*co*-nBA)-95, and P(DiPF-*co*-nBA)-78, almost constant values were observed for the α- and β-relaxation temperatures (Fig. 5b). For these three samples, the α-relaxation process was very weak. The data from P(DiPF-*co*-nBA)-64 were fundamentally different. From the tan δ, there were two strong relaxation processes with peak temperatures at 84 °C and 30 °C.

To further clarify the features of the chain dynamics of the DiPF copolymers, their thermal properties were recorded. Figure 6 depicts traces for the DSC measurements of PDiPF and of the copolymers. DSC captured the change in the heat capacity as a step in the heat flow curve. When the relaxation process caused a detectable change in heat capacity, this event was recorded by DSC. Typically, only a single glass transition, which is associated with the α-relaxation process, is detected for common polymers including polyacrylates and polymethacrylates [2]. Although less common, some studies have detected β-relaxation from calorimetry [47]. Here, we exclusively used T_{DSC} to represent relaxations observed by DSC because it was difficult to distinguish the mode of the chain dynamics based only on the calorimetric experimental results. Interestingly, PDiPF showed a clear step in the heat flow curve, which corresponded to the β relaxation temperature observed by DMA. This is a unique feature of PDiPF. This implies that the strong β-relaxation of DiPF segment causes the change in heat capacity. It was difficult to detect any α relaxation process of PDiPF by DSC under the present conditions. The thermal decomposition of the polymer actually occurred at a high temperature. To protect the instruments, other scans were made for the copolymers in a temperature range clearly below the decomposition temperature. Figures 6a and 6b present the results from P(DiPF-*co*-AdA)s and P(DiPF-*co*-nBA)s, respectively. As the PDiPF content decreased, the T_{DSC} of P(DiPF-*co*-AdA)s increased. For example, the samples with 100%, 65%, and 46% PDiPF content showed a T_{DSC} of 66 °C, 105 °C, and 114 °C, respectively. In contrast, the T_{DSC} of P(DiPF-*co*-nBA)s decreased as the PDiPF content decreased. The T_{DSC} values of P(DiPF-*co*-nBA)-64, P(DiPF-*co*-nBA)-35, and P(DiPF-*co*-nBA)-19 were 58 °C, −17 °C, and −53 °C, respectively.

The relaxation temperatures obtained from DMA and DSC are summarized in Table 1 and Fig. 7. In the case of P(DiPF-*co*-AdA)s, the T_{DSC} increased almost linearly as the PDiPF content decreased. According to the Fox equation [48], the T_g of a binary random copolymer can be estimated by the following equation:

$$1/T_g = x_1/T_{g,1} + (1 - x_2)/T_{g,2}. \quad (1)$$

Here, x indicates the composition of the two polymers denoted as 1 and 2. The calculated T_g from the Fox equation was plotted as a black line in Fig. 7. It is emphasized that for the samples containing more than 76% DiPF content, the

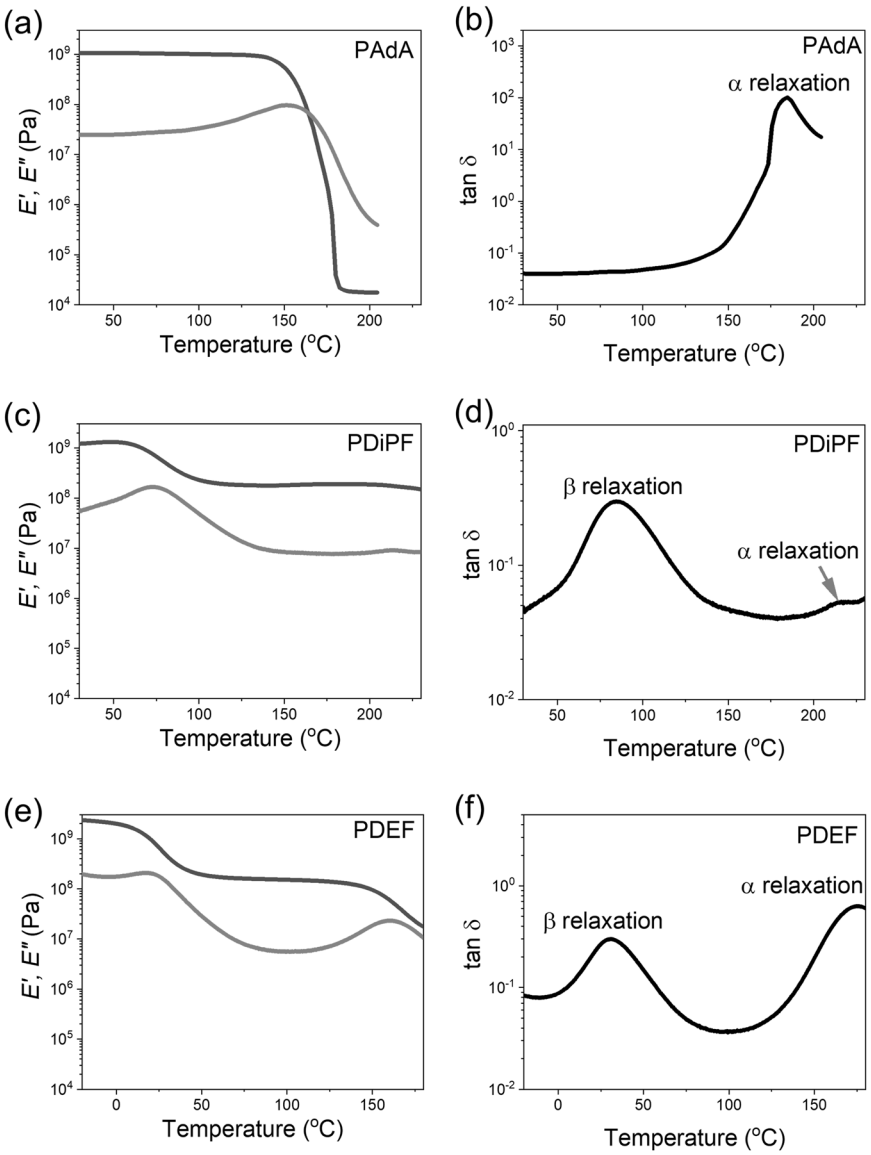

Fig. 3 Dynamic mechanical analysis (DMA) of poly(1-adamantyl acrylate) (PAdA) (**a** and **b**), poly(diisopropyl fumarate) (PDiPF) (**c** and **d**), and poly(diethyl fumarate) (PDEF) (**e** and **f**). *E′*, *E″* (**a**, **c**, and **e**) and tan δ (**b**, **d**, and **f**) are plotted as a function of time. The α-process of PDiPF is indicated with a gray arrow in **d**

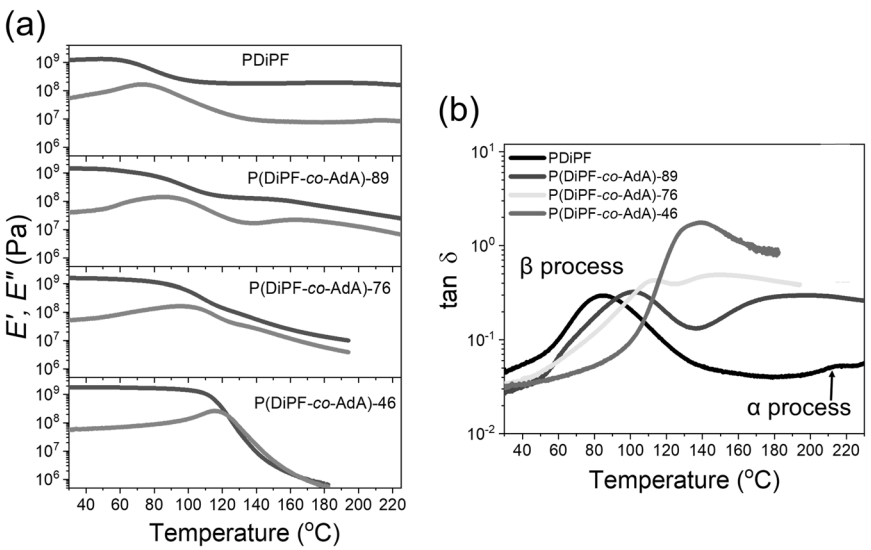

Fig. 4 Selected dynamic mechanical analysis (DMA) data from poly(diisopropyl fumarate) (PDiPF) and P(DiPF-*co*-AdA)s with different copolymer compositions. **a** Storage modulus (gray) and loss modulus (red) are plotted as a function of temperature. **b** Tan δ is plotted as a function of temperature. The number after the name of copolymer indicates the PDiPF content in the copolymer

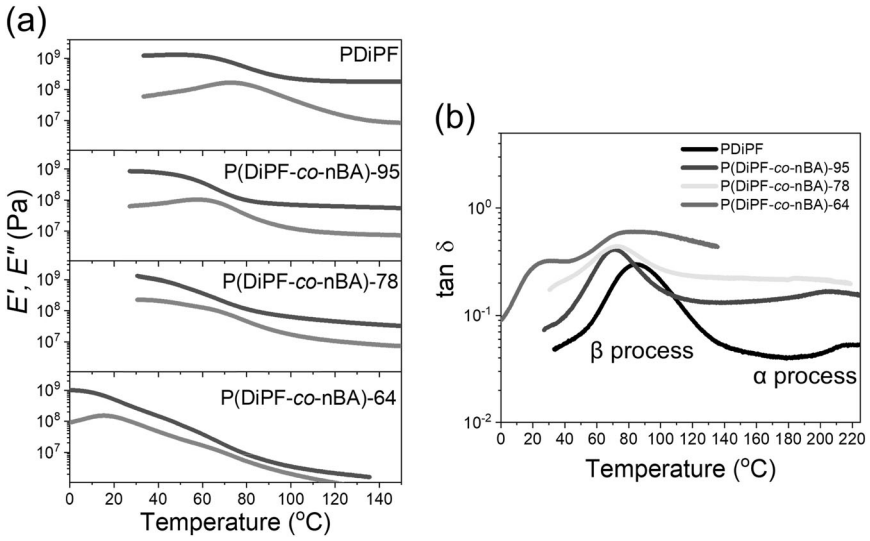

Fig. 5 Selected dynamic mechanical analysis (DMA) data from poly(diisopropyl fumarate) (PDiPF) and P(DiPF-*co*-nBA)s with different copolymer compositions. **a** Storage modulus (gray) and loss modulus (red) are plotted as a function of temperature. **b** Tan δ is plotted as a function of temperature. The number after the name of copolymer indicates the PDiPF content in the copolymer

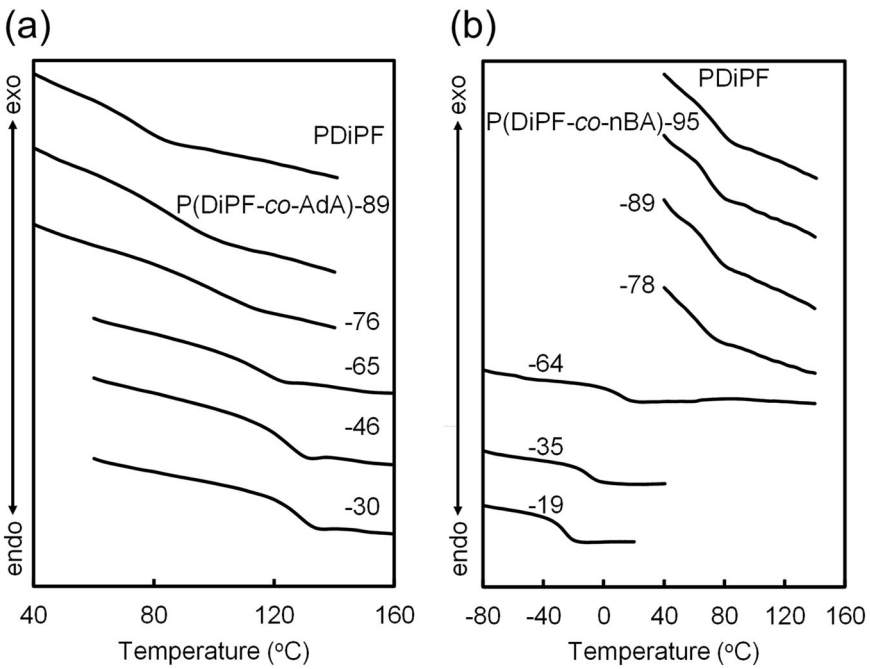

Fig. 6 Differential scanning calorimetry (DSC) curves of selected P(DiPF-*co*-AdA)s and P(DiPF-*co*-nBA)s with different copolymer compositions. The data were recorded upon heating with a rate of 10 °C/min

relaxation detected by DSC coincides with the β-relaxation measured by DMA. In contrast to the β-relaxation, the weak α-relaxation temperature decreased as the DiPF content decreased. Eventually, these two relaxation processes merged when the DiPF content was 46%. Figure 6b shows the relaxation temperatures for P(DiPF-*co*-nBA)s. Again, the β-relaxation process from PDiPF and the α-relaxation process followed the Fox equation. As the DiPF content decreased, both the α-relaxation and β-relaxation temperatures decreased. The α-relaxation temperature decreased significantly when the DiPF content decreased from 78 to 64%. This behavior suggests the merging of the α- and β-relaxation, and further investigation of the molecular dynamics observed during the α- and β-relaxation processes are now discussed.

Figure 8 displays selected DMA data of P(DiPF-*co*-AdA)-89 and P(DiPF-*co*-nBA)-89 measured at five different frequencies in a range from 0.5 to 10 Hz. The tan δ of the β-relaxation processes shows a clear maximum, while that of the α-relaxation processes was broad. Assuming the Arrhenius dependence of the β-relaxation processes, apparent activation energies were obtained (Table 1). It should be noted that an α-relaxation time (τ) as a function of temperature (T) generally follows the Vogel–Fulcher–Tammann equation [2]:

$$\tau = \tau_0 \exp\left(\frac{B}{T - T_0}\right), \quad (2)$$

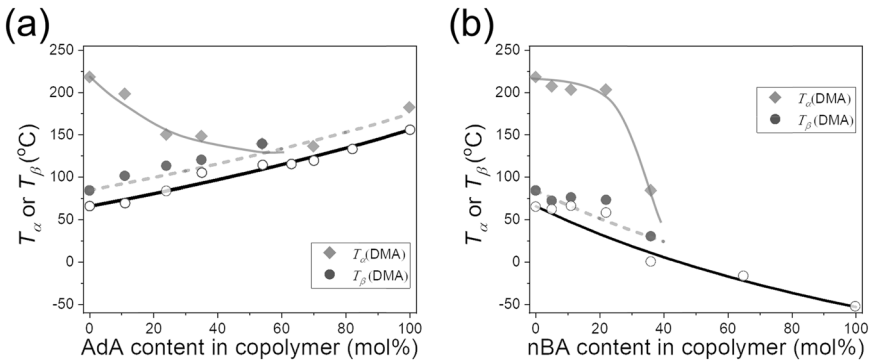

Fig. 7 Summary of the relaxation temperatures of **a** P(DiPF-*co*-AdA)s and **b** P(DiPF-*co*-nBA)s as a function of copolymer compositions. The filled symbols are from the dynamic mechanical analysis (DMA) data. The empty circles are from the differential scanning calorimetry (DSC) data. The black lines are predicted by the Fox equation. Red lines and dotted gray lines are visual aids

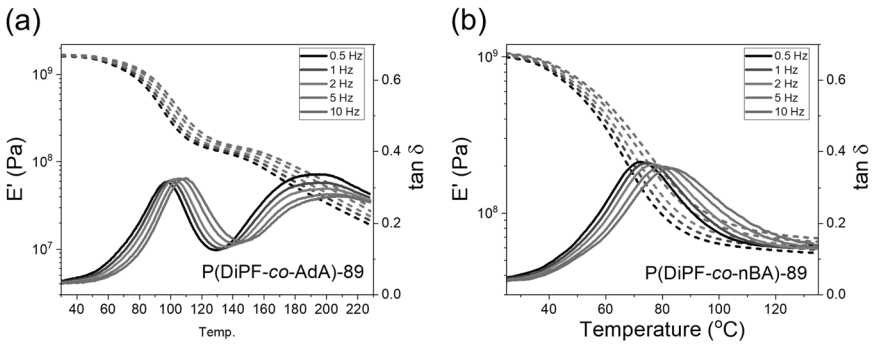

Fig. 8 Selected dynamic mechanical analysis (DMA) data from P(DiPF-*co*-AdA)-89 and P(DiPF-*co*-nBA)89 measured at 0.5, 1, 2, 5, and 10 Hz. Storage modulus (dotted line) and tan δ (line) as a function of temperature are plotted

where τ_0 is the relaxation at the high temperature limit, B is a positive constant, and T_0 is the ideal glass transition temperature. The characteristic time approaches infinity at T_0. The current frequency range (0.5–10 Hz) was too narrow to accurately fit the data (see Fig. S2 in the Supporting Information). The β-relaxation activation energy was 270 and 280–310 kJ/mol for PDiPF and the DiPF copolymers, respectively. The standard deviation of the fit was approximately ±10 kJ/mol. The literature activation energy values are 58–125 kJ/mol for the β-relaxation and 325–585 kJ/mol for the α-relaxation of PMMA [2, 16, 49–59], 59–63 kJ/mol for the β-relaxation and 180–238 kJ/mol for the α-relaxation of poly(methyl acrylate) (PMA) [54], and 113–152 kJ/mol for the β-relaxation and 210–294 kJ/mol for the α relaxation of PAdA and its block copolymers [33], as summarized in Table 2. Thus, the β-relaxation activation energy of PDiPF is much larger than that of conventional polyacrylates and polymethacrylates, but the frequency range investigated in this study was limited. A detailed analysis of the β-relaxation containing the fumarate segments is ongoing [60, 61].

Our results indicate the unique properties of β-relaxation arising from DiPF segments. This process is categorized as the relaxation due to side-chain motion. On the other hand, the fact that clear transition behavior was detected by DSC implies that this dynamic has some similarity with common α-relaxations for any other conventional vinyl polymers. These unique properties should be associated with hindered rotational motion due to the absence of a methylene group.

Table 2 List of activation energies estimated for some acrylic polymers in the literature

Polymers	Relaxation	E_{act} (kJ/mol)	Method	Ref.
PMMA	α	334, 325–343	DMA	[49, 50]
PMMA	α	376–585, 460	DS	[51, 52]
PMMA	β	75, 78	DMA	[16, 50]
PMMA	β	79, 81, 84, 96, 112	DS	[52–56]
PMMA	β	121	DMA/DS	[57]
PMMA	β	58, 125	FFM	[58, 59]
PMA	α	180, 238	DS	[52, 54]
PMA	β	59, 63	DS	[52, 54]
PAdA	α	292	DMA	[33]
PAdA/PnBA block copolymers	α	210–294	DMA	[33]
PAdA/PnBA block copolymers	β	113–152	DMA	[33]

PMMA poly(methyl methacrylate), *PMA* poly(methyl acrylate), *PAdA* poly(1-adamantyl acrylate), *PnBA* poly(*n*-butyl acrylate), *DMA* dynamic mechanical analysis, *DS* dielectric spectroscopy, *FFM* friction force microscopy

As shown in the case of PMMA [18], the β-relaxation of PDiPF may be a local step for the segmental motion associated with the α-relaxation.

Conclusion

We synthesized the DiPF homopolymer and two series of random copolymers containing DiPF and acrylates with several compositions. As counterpart acrylates, nBA and AdA whose glass transition temperatures are distinctively different were selected. The DMA measurement of PDiPF as the homopolymer showed a strong β-relaxation. The storage modulus decreased from ~1 GPa to ~0.1 GPa during the β-relaxation process. In both cases of copolymers of DiPF with AdA and nBA, we found that the β-relaxation from the DiPF segments and the α-relaxation from the polyacrylates segments were correlated with each other and merged according to the copolymer compositions. It was demonstrated that the random copolymerization of DiPF and acrylates enabled the control of both α- and β-relaxation processes for flexible and nonflexible polymer chains. Because the control of the dynamics of PDiPF by random copolymerization may open new application areas using side-chain dynamics, further characterization of the β-relaxation of PDiPF as well as some polymers containing DiPF repeating units is ongoing [60, 61].

Compliance with ethical standards

Conflict of interest The authors declare that they have no conflict of interest.

Publisher's note: Springer Nature remains neutral with regard to jurisdictional claims in published maps and institutional affiliations.

References

1. Brandrup J, Immergut EH, Grulke EA. Polymer handbook. New York: Wiley; 2003.
2. McCrum NG, Read BE, Williams G. An elastic and dielectric effects in polymeric solids. New York: Wiley; 1967.
3. Kahle S, Korus J, Hempel E, Unger R, Höring S, Schröter K, et al. Glass-transition cooperativity onset in a series of random copolymers poly(*n*-butyl methacrylate-stat-styrene). Macromolecules. 1997;30:7214–23.
4. Otsu T, Yasuhara T, Matsumoto A. Synthesis, characterization, and application of poly(substituted methylene)s. J Macromol Sci Chem. 1988;A25:537–54.
5. Matsumoto A, Maeo N, Sato E. Living radical polymerization of diisopropyl fumarate to obtain block copolymers containing rigid poly(substituted methylene) and flexible polyacrylate segments. J Polym Sci Part A. 2016;54:2136–47 and the references cited therein.
6. Otsu T, Ito O, Toyoda N, Mori S. Polymers from 1,2-disubstituted ethylenic monomers. 2. Homopolymers from dialkyl fumarates by radical initiator. Makromol Chem Rapid Commun. 1981;2:725–8.
7. Toyoda N, Otsu T. Polymers from 1,2-disubstituted ethylenic monomers. IX. Radical high polymerization of methyl-*tert*-butyl fumarate. J Macromol Sci Chem. 1983;19:1011–21.
8. Otsu T, Shiraishi K, Matsumoto A. Radical polymerization and copolymerization reactivities of fumarates bearing different alkyl ester groups. J Polym Sci Part A. 1993;31:2523–9.
9. Otsu T, Yasuhara T, Shiraishi K, Mori S. Radical high polymerization of di-*tert*-butyl fumarate and novel synthesis of high molecular weight poly(fumaric acid) from its polymer. Polym Bull. 1984;12:449–56.
10. Matsumoto A, Tarui T, Otsu T. Dilute solution properties of semiflexible poly(substituted methylenes): Intrinsic viscosity of poly(diisopropyl fumarate) in benzene. Macromolecules. 1990;23:5102–5.
11. Matsumoto A, Nakagawa E. Evaluation of chain rigidity of poly (diisopropyl fumarate) from light scattering and viscosity in tetrahydrofuran. Eur Polym J. 1999;35:2107–13.
12. Nakatsuji M, Hyakutake M, Osa M, Yoshizaki T. Mean-square radius of gyration and second virial coefficient of poly(diisopropyl fumarate) in dilute solution. Polym J. 2008;40:566–71.
13. Nakatsuji M, Soutoku K, Osa M, Yoshizaki T. Transport coefficients of poly(diisopropyl fumarate) in dlute solution. Polym J. 2009;41:83–9.
14. Gotze W, Sjogren L. Relaxation processes. Rep Prog Phys. 1992;55:241–376.
15. Kremer F, Schönhals A. Broadband dielectric spectroscopy. Berlin, Heidelberg: Springer; 2003.
16. Muzeau E, Perez J, Johari GP. Mechanical spectrometry of the β-relaxation in poly(methyl methacrylate). Macromolecules. 1991;24:4713–23.
17. Gun'ko VM, Zarko VI, Goncharuk EV, Andriyko LS, Turov VV, Nychiporuk YM, et al. TSDC spectroscopy of relaxational and interfacial phenomena. Adv Colloid Interface Sci. 2007;131:1–89.
18. Kulik AS, Beckham HW, Schmidt-Rohr K, Radloff D, Pawelzik U, Boeffel C, et al. Coupling of α and β processes in poly(ethyl methacrylate) investigated by multidimensional NMR. Macromolecules. 1994;27:4746–54.
19. Sondhauß J, Lantz M, Gotsmann B, Schirmeisen A. β-relaxation of PMMA: tip size and stress effects in friction force microscopy. Langmuir. 2015;31:5398–405.
20. Victor JG, Torkelson JM. On measuring the distribution of local free volume in glassy polymers by photochromic and fluorescence techniques. Macromolecules. 1987;20:2241–50.
21. Ngai KL, Paluch M. Classification of secondary relaxation in glass-formers based on dynamic properties. J Chem Phys. 2004;120:857–73.
22. Schmidt-Rohr K, Kulik AS, Beckham HW, Ohlemacher A, Pawelzik U, Boeffel C, et al. Molecular nature of the β relaxation in poly(methyl methacrylate) investigated by multidimensional NMR. Macromolecules. 1994;27:4733–45.
23. Yamada K, Takayanagi M, Murata Y. Relations between molecular aggregation state and mechanical properties in poly(diisopropyl fumarate). Polymer. 1986;27:1054–7.
24. Kurosu H, Yamada T, Ando I, Sato K, Otsu T, An NMR. study of structure and dynamics of poly(fumarate)s in the solid state. J Molec Struct. 1993;300:303–11.
25. Choi SB, Takahara A, Amaya N, Murata Y, Kajiyama T. Effects of ester side chain structure on gas permeation behavior of poly (dialkyl fumarate)s. Polym J. 1989;21:433–8.
26. Choi SB, Takahara A, Amaya N, Murata Y, Kajiyama T. Effect of ester side chains on the aggregation state and surface properties of poly(dialkyl fumarate)s. Polym J. 1989;21:215–9.
27. Shiraishi K, Sugiyama K. Liquid crystalline polymers from fumarates containing mesogenic methoxyphenylazophenoxy groups. Chem Lett. 1990;19:1697–700.

28. Noguchi H, Michinobu T, Shigehara K. Synthesis and the phase behavior of liquid-crystalline fumarates bearing tolane-based mesogens. Chem Lett. 2007;36:1044–5.
29. Shiraishi K, Sugiyama K, Sakamoto A, Otsu T. Nematic fumaric ester derivatives and their electro-optical properties. Bull Chem Soc Jpn. 1988;61:783–6.
30. Park K, Kikuchi H, Kajiyama T. Component dependence of aggregation structure and light scattering properties of polymer/liquid crystal composite films. Polym J. 1994;26:895–904.
31. Jeong HK, Kikuchi H, Kajiyama T. Low voltage light switching of hybrid-type cell composed of (polymer/liquid crystal) composite system. Polym J. 1997;29:165–70.
32. Jeong HK, Kikuchi H, Kajiyama T. (Polymer/liquid crystal) composite films with high electric charge holding. Chem Lett. 1999;28:1159–60.
33. Nakano Y, Sato E, Matsumoto A. Synthesis and thermal, optical, and mechanical properties of sequence-controlled poly(1-adamantyl acrylate)-block-poly(*n*-butyl acrylate) containing polar side group. J Polym Sci Part A. 2014;52:2899–910.
34. Matsumoto A, Sumihara T. Thermal and mechanical properties of random copolymers of diisopropyl fumarate with 1-adamantyl and bornyl acrylates with high glass transition temperatures. J Polym Sci Part A. 2017;55:288–96.
35. Otsu T, Yamada B, Ishikawa T. Determination of absolute rate constants for elementary reactions in radical polymerization of diethyl fumarate. Macromolecules. 1991;24:415–9.
36. Matsumoto A, Sano Y, Yoshioka M, Otsu T. Kinetic study of radical polymerization of dialkyl fumarates using electron spin resonance spectroscopy. J Polym Sci Part A. 1996;34:291–9.
37. Yamada B, Yoshikawa E, Shiraishi K, Miura H, Otsu T. Determination of absolute rate constants for radical polymerization of diisopropyl fumarate based on a quantitative scavenge of propagating radical. Polymer. 1991;32:1892–6.
38. Matsumoto A, Tanaka S, Otsu T. Synthesis and characterization of poly(1-adamantyl methacrylate): effects of the adamantyl group on radical polymerization kinetics and thermal properties of the polymer. Macromolecules. 1991;24:4017–24.
39. Otsu T, Matsumoto A, Horie A, Tanaka S. Synthesis of thermally stable vinyl polymers from adamantyl-containing acrylic derivatives. Chem Lett. 1991;20:1145–8.
40. Cypcar CC, Camelio P, Lazzeri V, Mathias LJ, Waegell B. Prediction of the glass transition temperature of multicyclic and bulky substituted acrylate and methacrylate polymers using the energy, volume, mass (EVM) QSPR model. Macromolecules. 1996;29:8954–9.
41. Hsiao S-H, Li C-T. Synthesis and characterization of new adamantane-bsed poyimides. Macromolecules. 1998;31:7213–7.
42. Liaw D-J, Liam B-Y. Synthesis and characterization of new polyamide-imides containing pendent adamantyl groups. Polymer. 2001;42:839–45.
43. Lu W, Huang C-L, Hong K-L, Kang N-G, Mays JW. Poly (1-adamantyl acrylate): living anionic polymerization, block copolymerization, and thermal properties. Macromolecules. 2016;49:9405–14.
44. Lu W, Yin P, Osa M, Wang W, Kang N-G, Hong K-L, et al. Solution properties, unperturbed dimensions, and chain flexibility of poly(1-adamantyl acrylate). J Polym Sci Part B. 2017;55:1526–31.
45. Ishizone T, Goseki R. Synthesis of polymers carrying adamantyl substituents in side chain. Polym J. 2018;50:805–19.
46. Kopesky ET, Haddad TS, McKinley GH, Cohen RE. Miscibility and viscoelastic properties of acrylic polyhedral oligomeric silsesquioxane-poly(methyl methacrylate) blends. Polymer. 2005;46:4743–52.
47. Fujimori H, Oguni M. Correlation index $(T_{g\alpha} - T_{g\beta})/T_{g\alpha}$ and activation energy ratio $\Delta\varepsilon_{a\alpha}/\Delta\varepsilon_{a\beta}$ as parameters characterizing the structure of liquid and glass. Solid State Commun. 1995;94:157–62.
48. Brostow W, Chiu R, Kalogeras IM, Vassilikou-Dova A. Prediction of glass transition temperatures: binary blends and copolymers. Mater Lett. 2008;62:3152–5.
49. Deutsch K, Hoff EAW, Reddish W. Relation between the structure of polymers and their dynamic mechanical and electrical properties. Part I. Some alpha-substituted acrylic ester polymers. J Polym Sci Part A General 1954;13:565–82.
50. Heijboer J. Molekulare Deutung sekundärer Dämpfungsmaxima. Kolloid Z. 1956;148:36–47.
51. Saito S, Nakajima T. Glass transition in polymers. J Appl Polym Sci. 1959;4:93–9.
52. Ishida Y. Studies on dielectric properties of polymethylacrylate. Kolloid Z. 1961;174:124–7.
53. Xie L, Huang X, Wu C, Jiang P. Core-shell structured poly (methyl methacrylate)/$BaTiO_3$ nanocomposites prepared by in situ atom transfer radical polymerization: a route to high dielectric constant materials with the inherent low loss of the base polymer. J Mater Chem. 2011;21:5897–906.
54. de Brouckere L, Offergeld G. The dielectric properties of solid polymers. J Polym Sci. 1958;30:105–18.
55. Ishida Y, Yamafuji K. Studies on dielectric behaviors in series of polyalkyl-methacrylates. Kolloid Z. 1961;177:97–116.
56. Garwe F, Schoenhals A, Lockwenz H, BeinerM, Schroeter K, Donth E. Influence of cooperative α dynamics on local β relaxation during the development of the dynamic glass transition in poly(*n*-alkyl methacrylate). Macromolecules. 1996;29:247–53.
57. Iwayanagi S, Hideshima T. Dynamical study on the secondary anomalous absorption region of polymethyl methacrylate. J Phys Soc Jpn. 1953;8:368–71.
58. Hammerschmidt JA, Gladfelter WL, Haugstad G. Probing polymer viscoelastic relaxations with temperature-controlled friction force microscopy. Macromolecules. 1999;32:3360–7.
59. Gauthier C. Schirrer time and temperature dependence of the scratch properties of poly(methylmethacrylate) surfaces. J Mater Sci. 2000;35:2121–30.
60. Miyata K, Fukao K, Suzuki Y, Matsumoto A. Dielectric relaxation of poly(diisopropyl fumartae). Polym Prep Jpn. 2019;68:3Pc041.
61. Suzuki Y, Miyata K, Sato M, Tsuji N, Fukao K, Matsumoto A. Unusual β relaxation of poly(diisopropyl fumarate) due to the absence of a methylene spacer in the main chain. In preparation.